

The NEROV Autonomous Underwater Vehicle

Thor I. Fossen and Jens G. Balchen

Department of Engineering Cybernetics
The Norwegian Institute of Technology (NTH)
N-7034 Trondheim, Norway

Abstract

The Norwegian Experimental Remotely Operated Vehicle (NEROV) is described. The vehicle is designed and built at the Department of Engineering Cybernetics, The Norwegian Institute of Technology (NTH). The NEROV vehicle is an unmanned autonomous underwater vehicle (AUV) especially designed for testing advanced intelligent and conventional control algorithms. The vehicle is autonomous with respect to both energy and information. The vehicle will also be used in the Modellbased Teleoperation (MOBATEL) project at NTH. In teleoperation it is desirable to remove the non-minimum phase behaviour i.e. the time delay in the communication channel caused by e.g. a hydroacoustic communication link. This suggests a modellbased control structure. The vehicle is currently being tested in the Towing Tank and the Ocean Basin Laboratory at the Norwegian Marine Technology Research Institute (MARINTEK) in Trondheim, Norway.

Introduction

Norway has long recognized the importance of the ocean to its economy, security and environment. Hence, Norway's economic interests are highly tied to areas such as oil and gas exploration, merchant shipping and the fisheries. We believe that the development of a new generation of unmanned underwater vehicles as well as underwater vehicle-manipulator systems will be crucial for oil and gas exploration. In particular as the costs of building and inspecting off-shore platforms and pipelines will drastically rise with increasing water depths. The use of divers in deep water is hazardous and limited due to obvious physiological limitations. Hence, it is desirable to limit the use of divers. As major developers of off-shore technology, Norwegian industry and research institutes have recognized the need for more advanced underwater vehicle systems. As a result of this, we have increased our activities in underwater robotics at the Norwegian Institute of Technology. Some of the research programmes on autonomous underwater vehicles in Norway are described in Rødseth (1990) while a description of the Norwegian research programme on advanced robotic systems is found in Egeland (1991).

The NEROV vehicle, Sagatun and Fossen (1991a), is

a result of this new research activity. The NEROV vehicle is built as an open frame housing three cylindrical containers where the batteries, sensors and the computer system are located. Six adjustable thrusters are mounted on the frame such that each thruster pair can be used to control one translational and rotational motion. Hence, the vehicle is controllable in all 6 degrees of freedom (DOF). A brief sketch of the NEROV vehicle is shown in Figure 1. The most important design criteria for the NEROV Vehicle were that the vehicle should be:

- inexpensive.
- controllable in 6 DOF. Testing and integrating of new control algorithms on the vehicle should be a routine matter.
- positive buoyant.
- designed for at least 100 m depth.
- built of standard off-the-shelf sensors, computer hardware, thrusters and energy sources.
- autonomous with respect to energy and information.
- easy to test for different thruster configurations.
- designed for dynamic positioning (DP) in 6 DOF. This requires symmetrical thrust.
- used in underwater robotic research e.g. teleoperation and graduate courses at the Norwegian Institute of Technology.

This paper is outlined as follows: the second section discusses the NEROV equations of motion. The next sections describe the NEROV propulsion, sensor and computer system, respectively. Finally, the NEROV control system is discussed. Compensation of current induced disturbances are emphasized. Our conclusions and recommendations for future work are given at the end of the paper.

The NEROV Equations of Motion

It is convenient to define the ROV state vectors according to the Society of Naval Architects and Marine Engineers (SNAME) notation. The body-fixed linear and angular velocity vector in surge, sway, heave, roll, pitch and yaw, is defined as: $\dot{\mathbf{q}} = (u, v, w, p, q, r)^T$, where \mathbf{q} is a virtual vector. The corresponding earth-fixed position and Euler angle vector is defined as:

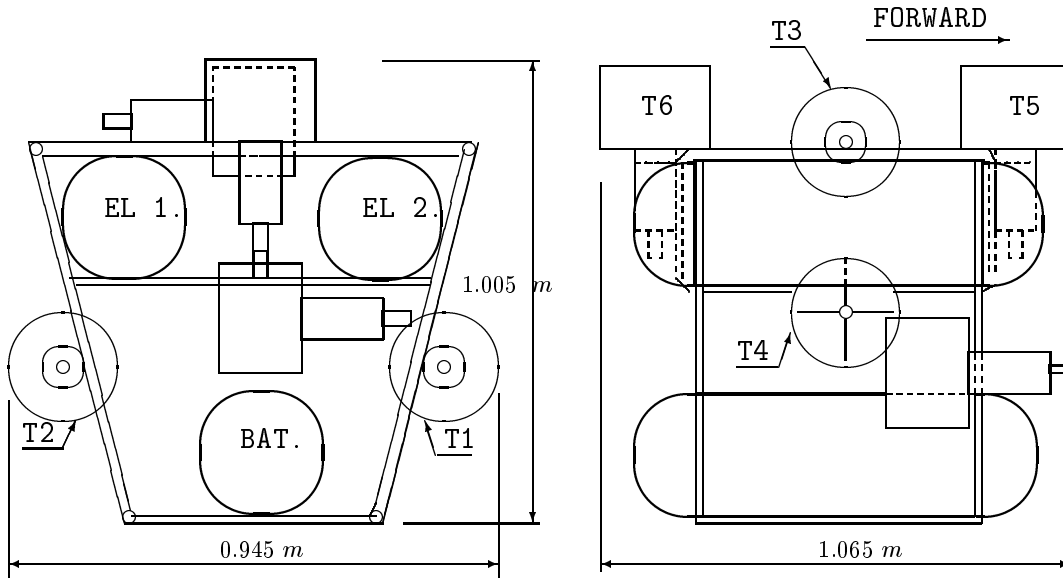


Figure 1: General arrangement of the NEROV vehicle.

$\mathbf{x} = (x, y, z, \phi, \theta, \psi)^T$. Further, let $\boldsymbol{\tau}$ be a vector of thruster forces and moments defined as

$$\boldsymbol{\tau} = \mathbf{B}(\dot{\mathbf{q}}) \mathbf{u}$$

where \mathbf{B} can be interpreted as a 6×6 velocity dependent thruster configuration matrix and \mathbf{u} is a vector of thruster inputs corresponding to thruster T1-T6 in Figure 1.

For the NEROV vehicle the local coordinate system is chosen to coincide with the vehicle's centre of gravity i.e. $\mathbf{r}_G = (0, 0, 0)^T$. The centre of buoyancy can be described as $\mathbf{r}_B = (x_B, 0, z_B)^T$. The most significant terms in the 6 DOF NEROV equations of motion are:

$$\begin{aligned} (m - X_{\ddot{u}})\ddot{u} - (m - Y_{\dot{v}})rv_r + (m - Z_{\dot{w}})qw_r = \\ X_u u_r + X_{u|u}|u_r| + \tau_1 \\ (m - Y_{\dot{v}})\ddot{v} + (m - X_{\ddot{u}})ru_r - (m - Z_{\dot{w}})pw_r = \\ Y_v v_r + Y_{v|v}|v_r| + \tau_2 \\ (m - Z_{\dot{w}})\ddot{w} - (m - X_{\ddot{u}})qu_r + (m - Y_{\dot{v}})pv_r = \\ Z_w w_r + Z_{w|w}|w_r| + \tau_3 \\ (I_x - K_{\dot{p}})\dot{p} + (Y_{\dot{v}} - Z_{\dot{w}})v_r w_r + (I_z - N_{\dot{r}})qr - (I_y - M_{\dot{q}})qr = \\ K_p p + K_{p|p}|p| + z_B B \cos \theta \sin \phi + \tau_4 \\ (I_y - M_{\dot{q}})\dot{q} - (X_{\ddot{u}} - Z_{\dot{w}})u_r w_r + (I_x - K_{\dot{p}})pr - (I_z - N_{\dot{r}})pr = \\ M_q q + M_{q|q}|q| + z_B B \sin \theta + x_B B \cos \theta \cos \phi + \tau_5 \\ (I_z - N_{\dot{r}})\dot{r} + (X_{\ddot{u}} - Y_{\dot{v}})u_r v_r - (I_x - K_{\dot{p}})pq + (I_y - M_{\dot{q}})pq = \\ N_r r + N_{r|r}|r| - x_B B \cos \theta \sin \phi + \tau_6 \end{aligned}$$

Here $u_r = u - u_f$, $v_r = v - v_f$ and $w_r = w - w_f$ are the relative velocity in surge, sway and heave, respectively. The subscript f denotes the fluid motion.

Sea currents may dramatically reduce the performance of the control system. We suggest including an adaptive feedforward term to compensate for slowly varying environmental disturbances. Hence, in the nonlinear underwater vehicle equations of motion, we assume that the earth-fixed current velocity components \dot{x}_f , \dot{y}_f and \dot{z}_f are constant or at least slowly varying.

Hence, the current velocity in the vehicle-fixed reference frame are

$$\begin{bmatrix} u_f \\ v_f \\ w_f \end{bmatrix} = \begin{bmatrix} c\psi c\theta & s\psi c\theta & -s\theta \\ -s\psi c\phi + c\psi s\theta s\phi & c\psi c\phi + s\phi s\theta s\psi & c\theta s\phi \\ s\psi s\phi + c\psi c\phi s\theta & -c\psi s\phi + s\theta s\psi c\phi & c\theta c\phi \end{bmatrix} \begin{bmatrix} \dot{x}_f \\ \dot{y}_f \\ \dot{z}_f \end{bmatrix}$$

We will also assume that all terms including components of the fluid velocity can be lumped together into a total current disturbance vector \mathbf{v} such that the nonlinear equations of motion can be expressed in a compact form as

$$\mathbf{M}\ddot{\mathbf{q}} + \mathbf{C}(\dot{\mathbf{q}})\dot{\mathbf{q}} + \mathbf{D}(\dot{\mathbf{q}})\dot{\mathbf{q}} + \mathbf{g}(\mathbf{x}) + \mathbf{v}(t) = \boldsymbol{\tau}$$

$$\dot{\mathbf{v}} = \boldsymbol{\eta}(t) \quad , \quad \boldsymbol{\eta}(t) \text{ is white noise}$$

$$\dot{\mathbf{x}} = \mathbf{J}(\mathbf{x})\dot{\mathbf{q}} \quad (1)$$

Here \mathbf{M} is a 6×6 inertia matrix including hydrodynamic added mass, \mathbf{C} is a 6×6 matrix of Coriolis, centrifugal and added mass coupling terms, \mathbf{D} is a 6×6 matrix of dissipative terms, such as potential damping, viscous damping and skin friction, \mathbf{g} is a 6×1 vector of restoring forces and moments and \mathbf{J} is a 6×6 transformation matrix, function of the Euler angles: ϕ , θ and ψ . These terms are described more closely in Fossen (1991).

The disadvantage of the assumption that disturbances can be linearly superpositioned in the nonlinear equations of motion is that model misalignments are imposed. However, simulations show that this is a good assumption.

The NEROV Propulsion System

The NEROV propulsion system is based on six 24 V 400 W permanent magnet motors which are made by the Outboard Marine Cooperation. By extending the

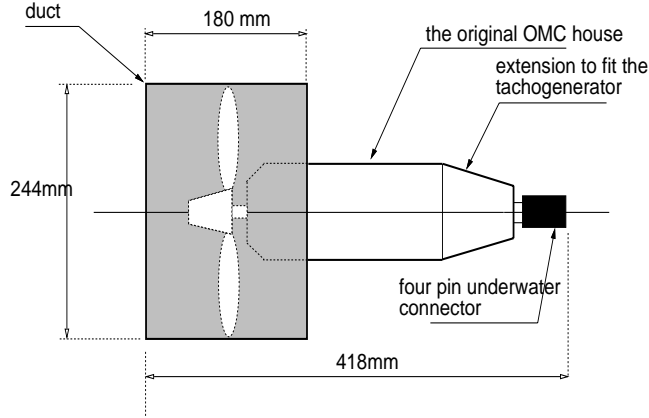


Figure 2: The NEROV ducted thruster.

motor house we were able to fit a tachogenerator inside the unit, see Fig. 2.

The tachogenerator was used to design an analog inner loop PID-controller. Consider the motor and regulator transfer functions

$$h_{motor}(s) = \frac{K}{(1 + T_1 s)(1 + T_2 s)}$$

$$h_{PID}(s) = \frac{K_P}{T_I s} \frac{(1 + T_I s)(1 + T_D s)}{1 + T_f s}$$

This suggests that the regulator time constants should be selected as $T_I = T_1$, $T_D = T_2$ and $T_f \approx 10 T_D$ which yields the loop transfer function

$$L(s) = h_{PID}(s) h_{motor}(s) = \frac{K_P K}{T_I s (1 + T_f s)}$$

Hence, excellent tracking and noise rejection is obtained. The thruster bandwidth can be improved by simply increasing the regulator gain K_P . A block diagram illustrating the inner loop feedback control system is shown in Fig. 3.

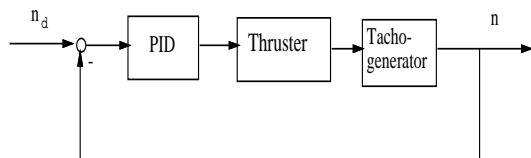


Figure 3: Block diagram of the inner loop feedback control system where n is the propeller angular velocity measurement and n_c is the commanded angular velocity.

We have also designed a duct for the thruster to increase the maximum thruster force. Experiments with a three bladed propeller (diameter 0.24m) of Kaplan type with radial pitch distribution showed that the maximum thruster force in Bollard pull was $T = 79N$, Sagatun and Fossen (1991b).

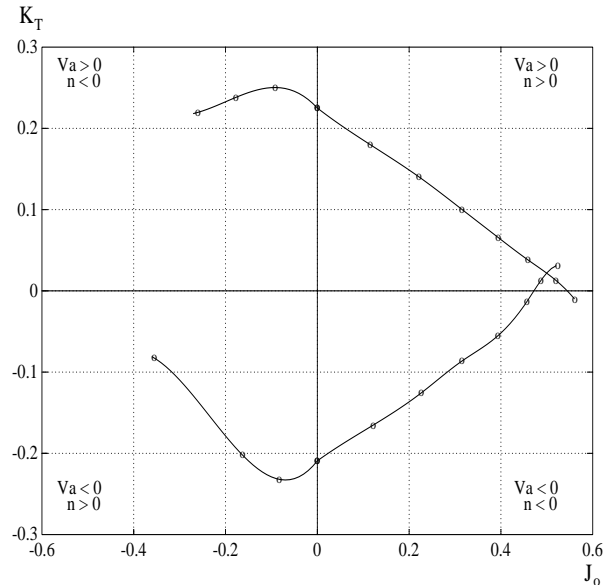


Figure 4: Experimental non-dimensional thrust coefficient K_T versus advance coefficient J_o for the NEROV thruster.

From the experimental data, the non-dimensional thrust coefficient

$$K_T = \frac{T}{\rho D^4 n |n|}$$

with ρ as the water density, n as the propeller revolution and D as the propeller diameter, was plotted against the advance coefficient J_o

$$J_o = \frac{V_A}{nD}$$

Here V_A is the advance velocity at the propeller. The results are shown in Figure 4. The experiments show that the thruster force is almost symmetrical, Sagatun and Fossen (1991b).

The NEROV Sensor System

The NEROV sensor system is based on the kinematic equations of motion which make the sensor system independent of the vehicle's hydrodynamic coefficients. The linear and angular state estimators were designed individually, see Figure 5.

For implementation simplicity, steady state diagonal Kalman filter gain matrices were used. The sampling frequencies are 10 Hz for the linear state estimator and 50 Hz for the angular state estimator, respectively. The bandwidth limitations are due to the measurement rate of the hydroacoustic system. The performance of the linear state estimator is shown in Figure 6.

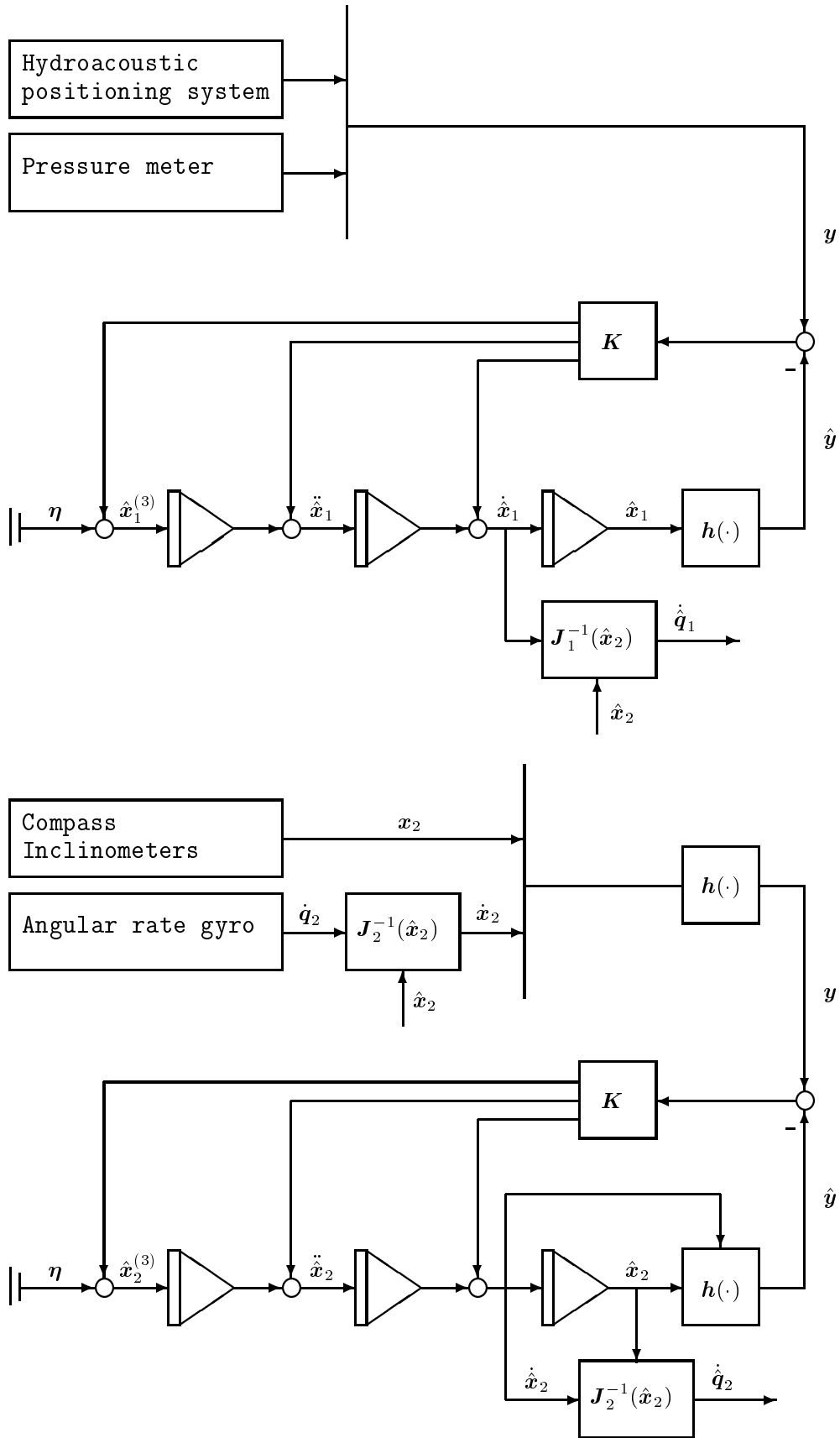


Figure 5: Linear and angular state estimators.

The computer system is based on the VMEbus and is located in one of the vehicle's upper containers. We used the single height Eurocard format due to the limited size of the vehicle's container. The processor board consists of one Motorola MC68020 32 bits 16 MHz microprocessor, one MC68881 floating point co-processor, 1 MByte of static RAM and 512 KBytes of ROM. The microprocessor card is fitted with two RS232 serial ports. These ports are used to connect a terminal and a monitor to the system while programming, testing and operating the computer system.

Besides these two computer cards take care of the I/O to and from the sensors and the propulsion system. We have currently sixteen 12 bits A/D input channels, eight TTL I/O ports and twelve A/D output channels. All I/O ports are programmable. The software is interrupt driven and is programmed in C on a SUN workstation and downloaded through a serial port to the VME rack. The NEROV computer system is described in (Sagatun and Fossen, 1991b).

The NEROV Control System

Conventional multivariable controllers are difficult to design for AUVs. This is because their strongly coupled dynamics are highly nonlinear and vary according to the vehicle's operating point. One of the design goals for the NEROV vehicle was that the vehicle should be able to perform highly coupled manoeuvres in all 6 DOF with some speed. Simulations show that this can be accomplished by applying nonlinear adaptive control theory. We will restrict our discussion to passivity-based adaptive control (PBAC) schemes. PBAC, Slotine and Li (1987), Sadegh and Horowitz (1987) and Kelly and Carelli (1988), exploit the skew symmetry property of $\dot{M} - 2C$, c.f. Ortega and Spong (1988). The parameter update laws in this section are based on an extension of the PBAC scheme of Slotine and Li (1987) and Slotine and Benedetto (1990) to underwater vehicles. Compensation of environmental disturbances is emphasized.

PBAC

Consider the equations of motion for an underwater vehicle which can be written as, Fossen (1991),

$$M^*(x)\ddot{x} + C^*(x, \dot{x})\dot{x} + D^*(x, \dot{x})\dot{x} + g^*(x) + v^*(x) = J^{-T}(x)\tau$$

where

$$\begin{aligned} M^*(x) &= J^{-T}MJ^{-1} \\ C^*(x, \dot{x}) &= J^{-T} [C - MJ^{-1}\dot{J}] J^{-1} \\ D^*(x, \dot{x}) &= J^{-T}DJ^{-1} \\ g^*(x) &= J^{-T}g \end{aligned}$$

Define a measure of tracking s as

$$s = \dot{\tilde{x}} + \lambda\tilde{x} \tag{2}$$

where λ is a strictly positive constant which may be interpreted as the control bandwidth and $\tilde{x} = x - x_d$ is the tracking error.

Let $\tilde{\theta} = \hat{\theta} - \theta$ be the parameter error vector and $\tilde{v} = \hat{v} - v$ be the current vector estimate error. The hat denotes the adaptive parameter estimates. Consider the Lyapunov-like function candidate

$$V(s, \tilde{\theta}, \tilde{v}, t) = \frac{1}{2}(s^T M^* s + \tilde{\theta}^T \Gamma \tilde{\theta} + \tilde{v}^T W \tilde{v})$$

where Γ and W are symmetric positive definite weighting matrices. Differentiating V with respect to time (assuming $M = M^T$) and using the skew symmetric property $\dot{s}^T(\dot{M}^* - 2C^*)\dot{s} = 0$ yields

$$\begin{aligned} \dot{V} &= -s^T D^* s + \dot{\tilde{\theta}}^T \Gamma \tilde{\theta} + \dot{\tilde{v}}^T W \tilde{v} \\ &\quad + s^T (J^{-T} \tau - M^* \ddot{x}_r - C^* \dot{x}_r - D^* \dot{x}_r - g^* - v^*) \end{aligned}$$

Fossen (1991) defines a virtual vector \dot{q}_r which satisfies the transformation

$$\dot{x}_r = J(x) \dot{q}_r$$

Hence, the virtual reference vectors \dot{q}_r and \ddot{q}_r can be calculated as

$$\begin{aligned} \dot{q}_r &= J^{-1}(x)\dot{x}_r \\ \ddot{q}_r &= J^{-1}(x)(\ddot{x}_r - \dot{J}(x)J^{-1}(x)\dot{x}_r) \end{aligned}$$

We now notice that the unknown terms M^* , C^* , D^* and g^* can be parameterized as

$$M^* \ddot{x}_r + C^* \dot{x}_r + D^* \dot{x}_r + g^* =$$

$$J^{-T} [M\ddot{q}_r + C\dot{q}_r + D\dot{q}_r + g] = J^{-T} \Phi(x, \dot{q}, \ddot{q}_r, \dot{q}_r) \theta$$

where θ is an unknown parameter vector and Φ is a known regressor matrix of appropriate dimensions. We have here assumed that the terms M , C , D and g are linear in their parameters. This yields

$$\dot{V} = -s^T D^* s + s^T J^{-T}(\tau - \Phi \theta - v) + \dot{\tilde{\theta}}^T \Gamma \tilde{\theta} + \dot{\tilde{v}}^T W \tilde{v}$$

Let the control law be chosen as

$$\tau = \Phi \hat{\theta} + \hat{v} - J^T K_D s \tag{3}$$

where $\hat{\theta}$ is the estimated parameter vector, \hat{v} is the estimated disturbance vector and K_D is a symmetric positive definite design matrix of appropriate. Then, the parameter update laws

$$\dot{\hat{\theta}} = -\Gamma^{-1} \Phi^T(x, \dot{q}, \ddot{q}_r, \dot{q}_r) J^{-1}(x) s \tag{4}$$

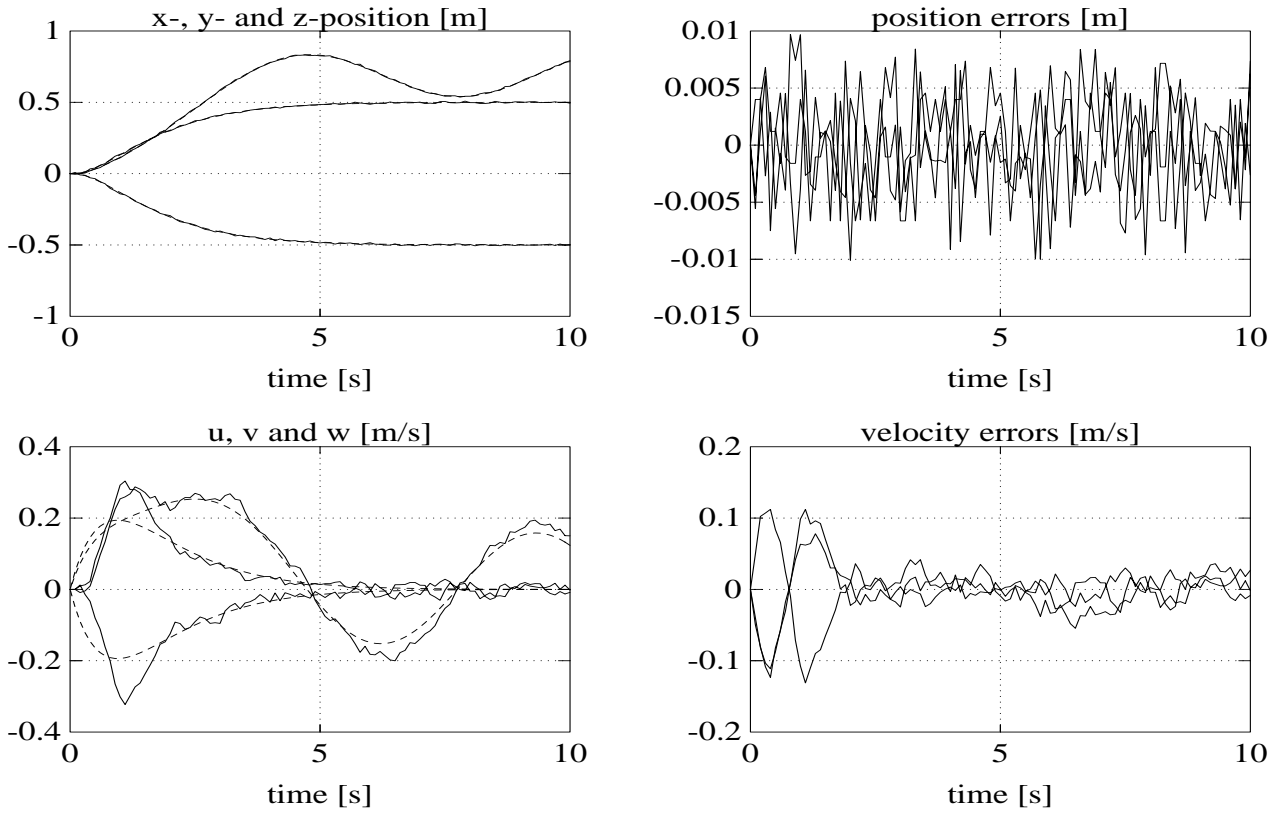


Figure 6: **Upper left:** actual (dotted) and estimated (solid) positions, **upper right:** position errors, **lower left:** actual (dotted) and estimated (solid) linear velocities and **lower right:** linear velocity errors.

$$\dot{\hat{\mathbf{v}}} = -\mathbf{W}^{-1}\mathbf{J}^{-1}(\mathbf{x})\mathbf{s} \quad (5)$$

yields

$$\dot{V} = -\mathbf{s}^T(\mathbf{K}_D + \mathbf{D}^*)\mathbf{s} \leq 0$$

This is due to the fact that the damping matrix $\mathbf{D} > 0$ implies that $\mathbf{D}^* = \mathbf{J}^{-T}\mathbf{D}\mathbf{J}^{-1} > 0$. Hence, Barbalat's Lyapunov-like lemma ensures that $\tilde{\boldsymbol{\theta}}$ is bounded and $\mathbf{s} \rightarrow 0$. This in turn implies that the tracking error vector $\tilde{\mathbf{x}} \rightarrow 0$.

VS-PBAC

An alternative parameter update law can be found by deriving a variable structure passivity-based adaptive controller (VS-PBAC). This approach was inspired by the variable structure model reference adaptive controller (VS-MRAC) of Tso *et al.* (1991). This scheme uses the parameterization of Craig (1988) which require both acceleration measurements and that the estimated inertia matrix is invertible. These limiting conditions may be removed by applying the parameterization of Slotine and Li (1987) instead. Thus we will show that it is straightforward to generalize the results of Tso *et al.* (1991) to the scheme of Slotine and Li (1987). Define a Lyapunov-like function candidate

$$V(\mathbf{s}, \tilde{\boldsymbol{\theta}}, t) = \frac{1}{2}\mathbf{s}^T\mathbf{M}^*\mathbf{s} \quad , \quad \mathbf{M}^* = (\mathbf{M}^*)^T > 0$$

Hence \dot{V} can be written as

$$\dot{V} = -\mathbf{s}^T\mathbf{D}^*\mathbf{s} + (\mathbf{J}^{-1}\mathbf{s})^T(\boldsymbol{\tau} - \boldsymbol{\Phi}\boldsymbol{\theta} - \mathbf{v})$$

Substituting the control law Eq. 3 into the expression for \dot{V} yields

$$\dot{V} = -\mathbf{s}^T(\mathbf{D}^* + \mathbf{K}_D)\mathbf{s} + (\mathbf{J}^{-1}\mathbf{s})^T(\boldsymbol{\Phi}\tilde{\boldsymbol{\theta}} + \tilde{\mathbf{v}})$$

We now notice that the last term in the expression for \dot{V} can be written as

$$(\mathbf{J}^{-1}\mathbf{s})^T\boldsymbol{\Phi}(\tilde{\boldsymbol{\theta}} - \boldsymbol{\theta}) = \sum_{i=1}^r(\hat{\theta}_i - \theta_i)(\boldsymbol{\Phi}^T\mathbf{J}^{-1}\mathbf{s})_i$$

$$(\mathbf{J}^{-1}\mathbf{s})^T(\tilde{\mathbf{v}} - \mathbf{v}) = \sum_{i=1}^r(\hat{v}_i - v_i)(\mathbf{J}^{-1}\mathbf{s})_i$$

Then, the parameter update laws

$$\dot{\hat{\theta}}_i = -\theta_i^m \operatorname{sgn}[(\boldsymbol{\Phi}^T\mathbf{J}^{-1}\mathbf{s})_i] \quad , \quad |\theta_i| \leq \theta_i^m$$

$$\dot{\hat{v}}_i = -v_i^m \operatorname{sgn}[(\mathbf{J}^{-1}\mathbf{s})_i] \quad , \quad |v_i| \leq v_i^m$$

yields $\dot{V} \leq 0$. Since $\|\boldsymbol{\Phi}\| < \infty$, Barbalat's Lyapunov-like lemma ensures that $\mathbf{s} \rightarrow 0$ and thus that the tracking error $\tilde{\mathbf{x}}$ converges to zero. A comparison study of the PBAC and the VS-PBAC is found in Fossen (1991)

Calculation of the Thruster Inputs

The control input vector is calculated as

$$\mathbf{u} = \mathbf{B}^{-1}(\dot{\mathbf{q}}) \boldsymbol{\tau}$$

where the non-zero elements in the input matrix are found as, Fossen (1991),

$$B_{ij} = \rho D^4 K_{T_{ij}}(J_o) \quad i = 1..6 \quad j = 1..6$$

Hence, the desired propeller revolution is given by $n_i = \text{sgn}(u_i)\sqrt{|u_i|}$. Uncertainties in the input matrix can be compensated by adding a discontinuous term to the adaptive control law. This is described more closely in Fossen and Sagatun (1991).

Dynamic Positioning of the NEROV vehicle

To illustrate the performance of the adaptive controller, dynamic positioning of the NEROV vehicle in surge and sway was considered. In the simulation study a 4 DOF model of NEROV vehicle was used,

$$\begin{aligned} (m - X_{\dot{u}})\dot{u} - (m - Y_{\dot{v}})rv_r &= X_u u_r + X_{u|u}|u_r| + \tau_1 \\ (m - Y_{\dot{v}})\dot{v} + (m - X_{\dot{u}})ru_r &= Y_v v_r + Y_{v|v}|v_r| + \tau_2 \\ (m - Z_{\dot{w}})\dot{w} &= Z_w w_r + Z_{w|w}|w_r| + \tau_3 \\ (I_z - N_{\dot{r}})\dot{r} + (X_{\dot{u}} - Y_{\dot{v}})u_r v_r &= N_r r + N_{r|r}|r| + \tau_6 \end{aligned}$$

The state vectors are recognized as $\mathbf{x} = (x, y, z, \psi)^T$ and $\dot{\mathbf{q}} = (u, v, w, r)^T$. An unknown current $\dot{x}_f = 0.9 [m/s]$, $\dot{y}_f = -0.8 [m/s]$ and $\dot{z}_f = 0.0 m/s$ was injected after 5 seconds. Hence,

$$\begin{bmatrix} u_f \\ v_f \\ w_f \end{bmatrix} = \begin{bmatrix} \cos \psi & \sin \psi & 0 \\ -\sin \psi & \cos \psi & 0 \\ 0 & 0 & 1 \end{bmatrix} \begin{bmatrix} \dot{x}_f \\ \dot{y}_f \\ \dot{z}_f \end{bmatrix}$$

The regressor matrix $\boldsymbol{\Phi}$ was based on the terms:

$$\mathbf{M} = \begin{bmatrix} m - X_{\dot{u}} & 0 & 0 & 0 \\ 0 & m - Y_{\dot{v}} & 0 & 0 \\ 0 & 0 & m - Z_{\dot{w}} & 0 \\ 0 & 0 & 0 & I_z - N_{\dot{r}} \end{bmatrix}$$

$$\mathbf{C} = \begin{bmatrix} 0 & -mr & 0 & Y_{\dot{v}}v_r \\ mr & 0 & 0 & -X_{\dot{u}}u_r \\ 0 & 0 & 0 & 0 \\ -Y_{\dot{v}}v_r & X_{\dot{u}}u_r & 0 & 0 \end{bmatrix}$$

$\mathbf{D} = -$

$$\begin{bmatrix} X_u + X_{u|u}|u_r| & 0 & 0 & 0 \\ Y_v + Y_{v|v}|v_r| & 0 & 0 & 0 \\ Z_w + Z_{w|w}|w_r| & 0 & 0 & 0 \\ N_r + N_{r|r}|r| & 0 & 0 & 0 \end{bmatrix}$$

$$\mathbf{J} = \begin{bmatrix} \cos \psi & -\sin \psi & 0 & 0 \\ \sin \psi & \cos \psi & 0 & 0 \\ 0 & 0 & 1 & 0 \\ 0 & 0 & 0 & 1 \end{bmatrix} \quad \mathbf{v} = \begin{bmatrix} v_1 \\ v_2 \\ v_3 \end{bmatrix}$$

$$\mathbf{B} = \rho D^4 \begin{bmatrix} K_{T11} & K_{T12} & 0 & 0 & 0 & 0 \\ 0 & 0 & -K_{T23} & K_{T24} & 0 & 0 \\ 0 & 0 & 0 & 0 & K_{T35} & K_{T36} \\ -l_1 K_{T11} & l_2 K_{T12} & 0 & 0 & 0 & 0 \end{bmatrix}$$

The adaptive control law, Eqs. 3-5, was simulated with $\mathbf{K}_D = \text{diag}(500, 500, 500, 250)$, $\boldsymbol{\Gamma} = 0.001 \mathbf{I}$, $\mathbf{W} = 0.001 \mathbf{I}$ and $\lambda = 1$. The NEROV vehicle was dynamically positioned in surge and sway ($x_d = 1$ and $y_d = 1 m$) while the depth was switched between $z_d = 2 m$ and $z_d = 3 m$. The desired heading angle was shifted between $\psi_d = \pm 30 \text{ deg}$. The sampling rate used in the simulation was 10 Hz. The desired outputs and the tracking errors are shown for both the PBAC and a PD-controller in Figure 7. Notice that there is a relatively small increase in the tracking error at $t = 5s$ where the current disturbances are injected. This shows that the PBAC yields high performance even for relative large constant disturbances. The simulations also verify that the model missalignments due the assumption that sea current disturbances could be linearly superpositioned in the nonlinear underwater vehicle equations of motion, hardly affects the performance of the controller. Indeed, the control law was found to be highly robust for errors in the regressor matrix.

Conclusions and Future Work

The NEROV vehicle has been described. This includes a brief discussion of the vehicle's equations of motion, thruster system, computer system, sensor system and control system. A simulation study of the vehicle's control system was performed to illustrate the robustness of the adaptive autopilot for unknown sea currents.

In the coming months a large number of full-scale experiments of the NEROV vehicle will be performed in the Ocean Basin Laboratory at MARINTEK. The PBAC will be implemented in late spring 1991. The full-scale experiments will include dynamic positioning in 6 DOF, heave compensation and tracking of general time-varying reference trajectories in 6 DOF. Pipeline tracking based on camera vision will also be investigated. The vehicle is also intended as a test bench for the MOBATEL telerobotic research programme at the Norwegian Institute of Technology which currently has 4 doctoral students.

Acknowledgments

This work was sponsored by the Royal Norwegian Council for Scientific and Industrial Research at the Center of Robotic Research at the Norwegian Institute of Technology (NTH).

The authors are grateful to Mr. Svein I. Sagatun at the Department of Engineering Cybernetics, NTH for his stimulating discussions and invaluable help in the design of the NEROV vehicle and to Mr. Erik Lehn at MARINTEK and Assistant Professor Bjørn Sortland at the Department of Marine Systems Design, NTH for their help with the open water test of the NEROV thruster and all the hydrodynamical tests of the vehicle.

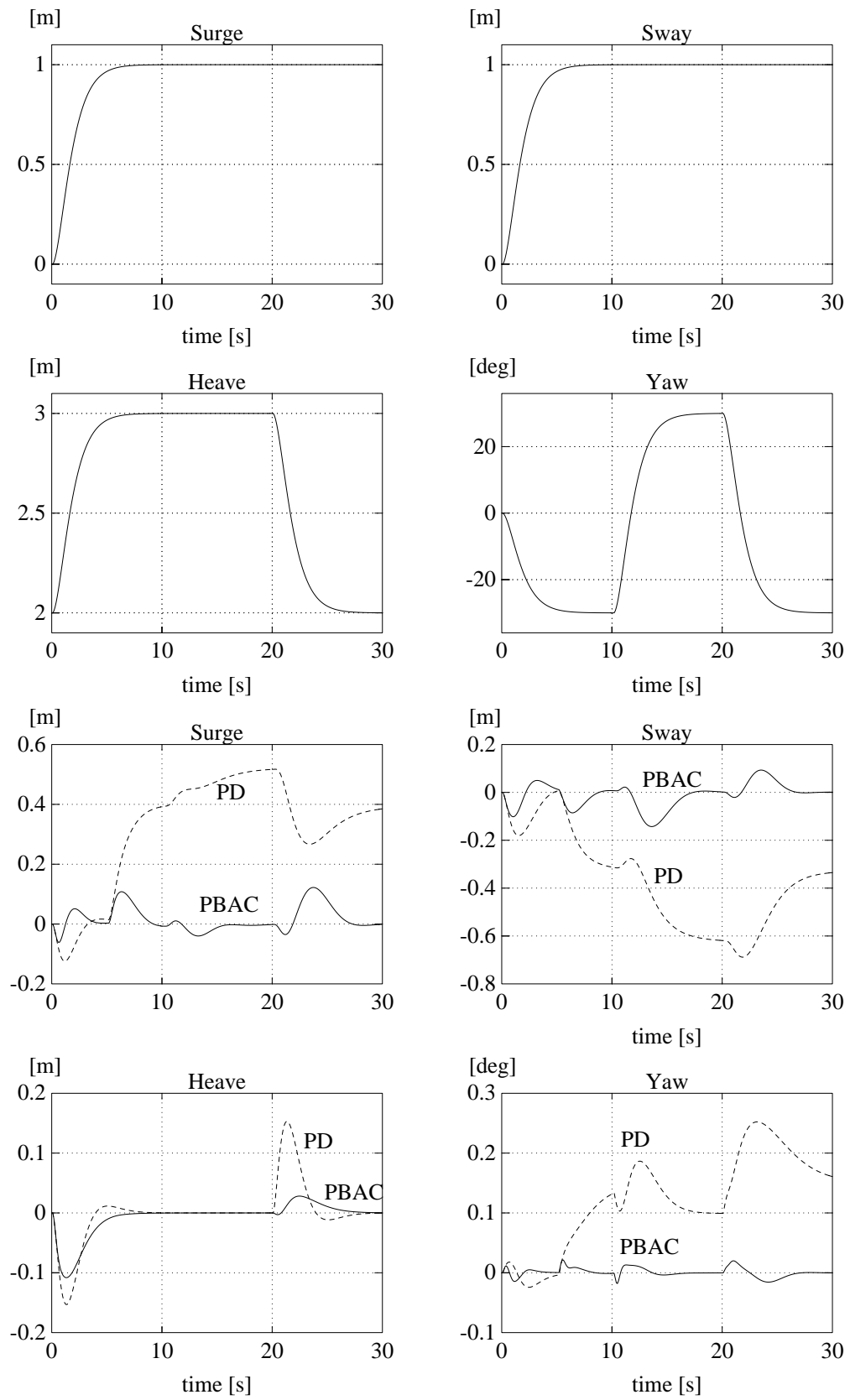


Figure 7: Desired outputs (upper plots) and tracking errors (lower plots) in surge, sway, heave and yaw.

References

- J. J. Craig (1988)**. *Adaptive Control of Mechanical Manipulators*. Addison-Wesley, Reading, Massachusetts.
- O. Egeland (1991)**. The Norwegian Research Programme on Advanced Robotic Systems. In *International Symposium on Advanced Robot Technology (ISART)*, Tokyo, Japan, March 1991.
- T. I. Fossen and S. I. Sagatun (1991)**. Adaptive Control of Nonlinear Underwater Robotic Systems. In *Proceedings of the IEEE Conference on Robotics and Automation*, pp. 1687–1695, Sacramento, California, April.
- T. I. Fossen (1991)**. Adaptive Macro-Micro Control of Nonlinear Underwater Robotic Systems. In *Proceedings of the 5th International Conference on Advanced Robotics (ICAR)*, pp. 1569–1572, Pisa, Italy, June.
- R. Kelly and R. Carelli (1988)**. Input-Output Analysis of an Adaptive Computed Torque plus Compensation Control for Manipulators. In *27th IEEE Conference on Decision and Control*, Austin, TX.
- R. Ortega and M. W. Spong (1988)**. Adaptive Motion Control of Rigid Robots: A Tutorial. In *Proceedings of the 27th Conference on Decision and Control*, pp. 1575–1584, Austin, TX.
- Ø. J. Rødseth (1990)**. Research on Autonomous Underwater Vehicles in Norway. In *Proceedings Seminar on Autonomous Underwater Vehicles, association for structural improvement of the shipbuilding industry*, Tokyo, Japan.
- N. Sadegh and R. Horowitz (1987)**. Stability Analysis of an Adaptive Controller for Robotic Manipulators. In *Proceedings of IEEE International Conference on Robotics and Automation*, pp. 1223–1229, Raleigh, North Carolina.
- S. I. Sagatun and T. I. Fossen (1991)**. The Norwegian Experimental Remotely Operated Vehicle (NEROV). In *Proceedings of the ROV'91 Conference*, Hollywood, Florida, May.
- S. I. Sagatun and T. I. Fossen (1991)**. The Norwegian Experimental Remotely Operated Vehicle (NEROV) Propulsion System. Technical Report 91-1-W, Division of Engineering Cybernetics, Norwegian Institute of Technology, N-7034 Trondheim, Norway.
- S. I. Sagatun and T. I. Fossen (1991b)**. The Norwegian Experimental Remotely Operated Vehicle (NEROV) Computer System. Technical Report 91-3-W, Division of Engineering Cybernetics, Norwegian Institute of Technology, N-7034 Trondheim, Norway.
- J. J. E. Slotine and M. D. Di Benedetto (1990)**. Hamiltonian Adaptive Control of Spacecraft. *IEEE Transactions on Automatic Control*, AC-35, No. 7, pp. 848–852.
- J. J. E. Slotine and W. Li (1987)**. Adaptive Manipulator Control. A Case Study. In *Proceedings of the 1987 IEEE Conference on Robotics and Automation*, pp. 1392–1400, Raleigh, North Carolina.
- S. K. Tso, Y. Xu, and H. Y. Shum (1991)**. Variable Structure Model Reference Adaptive Control of Robot Manipulators. In *Proceedings of IEEE International Conference on Robotics and Automation*, pp. 2148–2153, Sacramento, California, April.